Supplementary material (ESI) for Journal of Materials Chemistry

Supporting Information

A Novel and Facile Solution-Phase Deposition Approach to Porous Selenium Materials

Bin Zhang,[a,b] *Xingchen Ye,*[a] *Chengming Wang*[a] *and Yi Xie**[a]

[a] *Department of Nanomaterials and Nanochemistry, Hefei National Laboratory for Physical Sciences at Microscale, University of Science and Technology of China, Hefei 230026, P. R. China. E-mail: yxie@ustc.edu.cn.*

[b] *School of Sciences, Tianjin University, Tianjin, 300072，P . R. China*

S1. Scheme illustrating the synthesis of selenium materials using the novel solution-phase deposition approach.

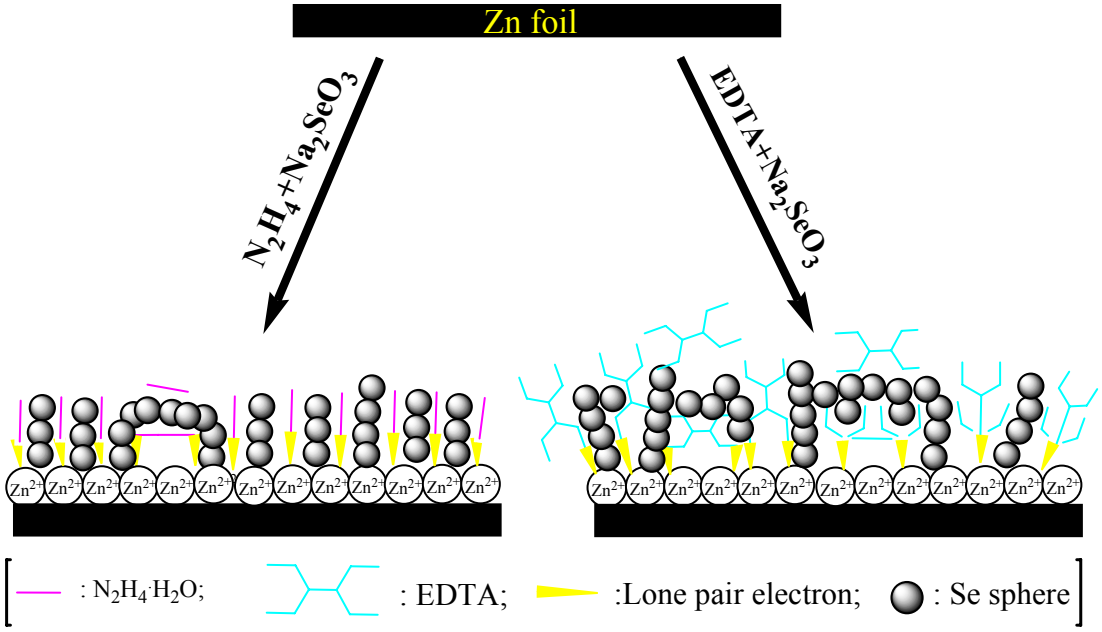

Figure S1-1. Scheme illustrating the synthesis of selenium materials using the novel solution-phase deposition approach. From this scheme, it is reasonable to except that the dimension-constrained role of different amine-containing molecules coordinated with metal ions may result in the differences in Se samples' morphologies.

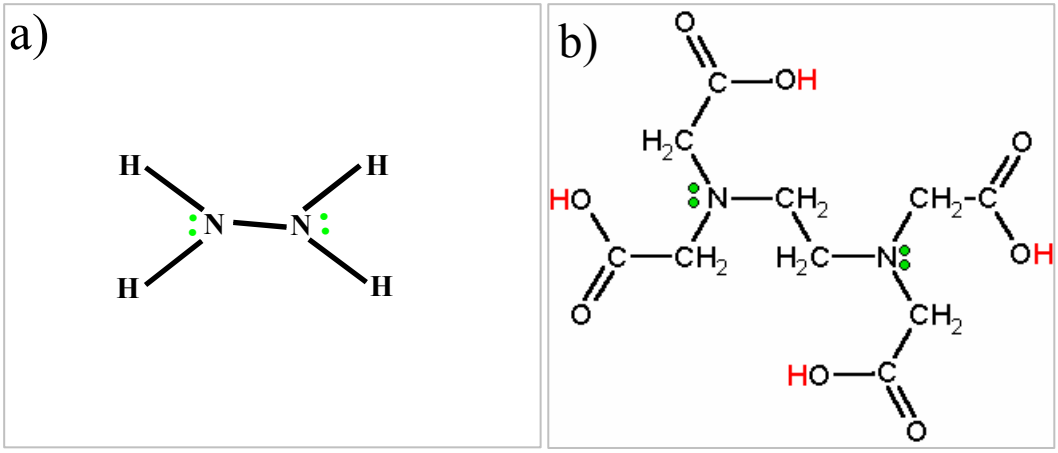

Figure S1-2. Scheme illustrating the structures of hydrazine hydrate and EDTA molecule.

S2. SEM images of the as-prepared porous flower-like Se patterns

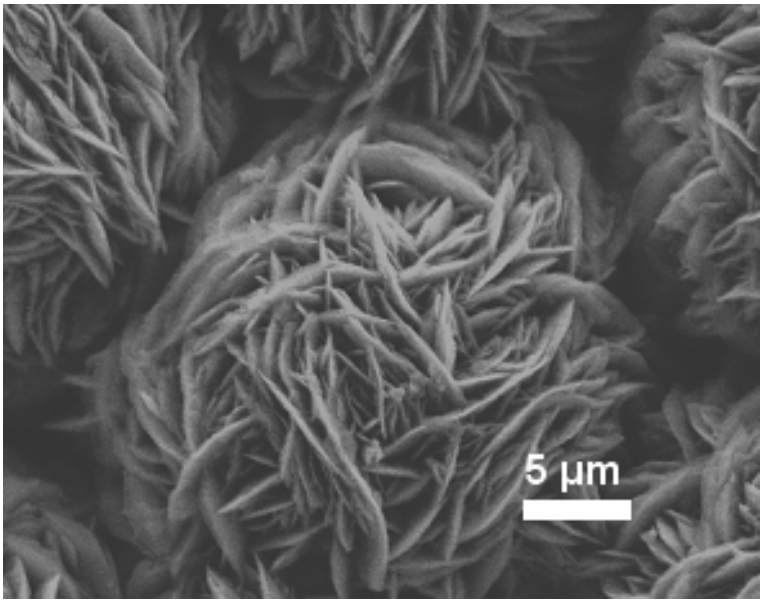

Figure S2. Higher magnification SEM image of porous flower-like Se patterns, indicating that the flower-like pattern is composed of nanoflakes with the thickness of ~300 nm.

S3. TEM images of the porous Se materials prepared by this facile solution-phase deposition method.

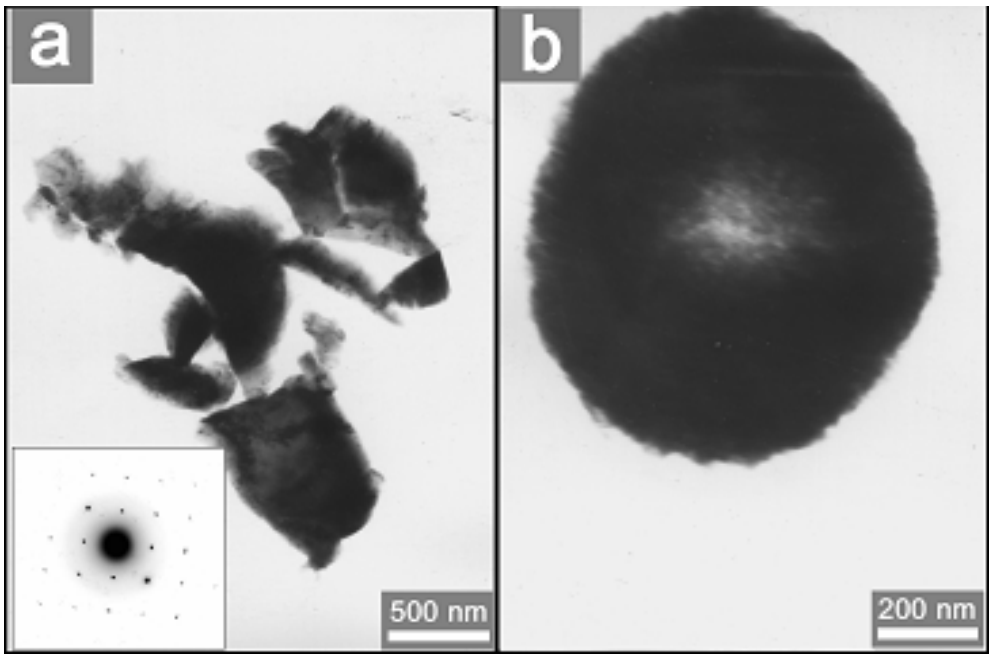

Figure S3. TEM images of porous flower-like Se patterns (a) and porous apple-like microspheres. The inset in Figure S3a is the SAED pattern. Figure S3a and the inset show that the flower-like patterns are composed of selenium with high crystallinity. Figure S3b indicate that the apple-like microspheres are hollow. Due to the samples' large size and instability of selenium when exposed to electron beam, it is difficult to discern the porous structure and obtain the SAED pattern.

S4. XRD patterns of the as-prepared porous selenium microspheres.

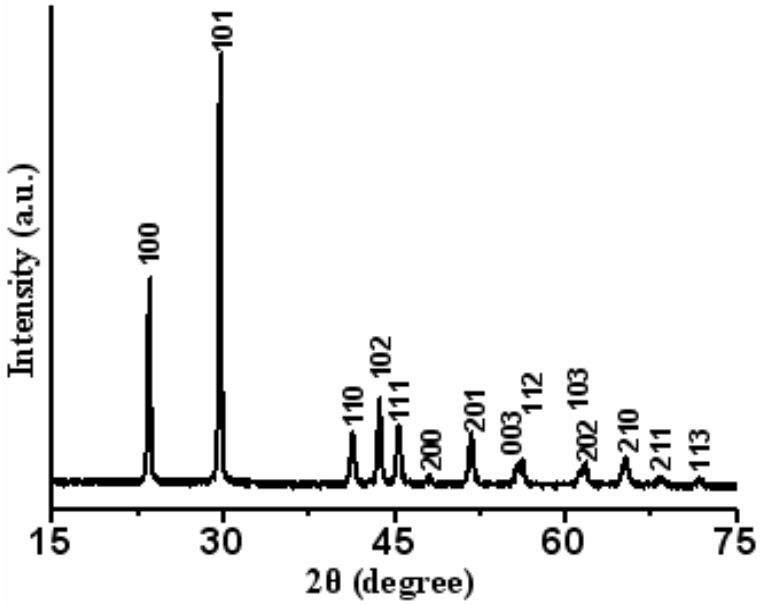

Figure S4. XRD pattern of the as-prepared porous apple-like Se microspheres. Different from that of Figure 2b, this porous Se sample is carefully scraped from the Zn substrates, and then washed three times each with dilute acid, water and absolute ethanol. This shows that the pure porous selenium samples can be easily separated from the substrate.

S5. Raman spectra of the as-prepared porous selenium products.

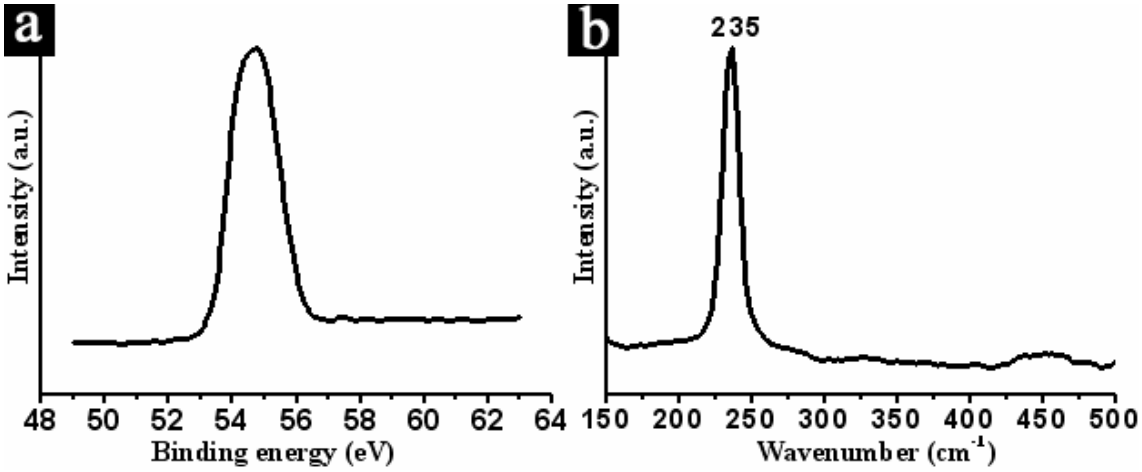

Figure S5. XPS (a) and Raman (b) spectra of the porous apple-like Se microspheres. In the XPS spectrum, the peak centered at 54.71 eV can be attributed to Se3d and no obvious peak from Se-O are observed, indicating the high purity of the products. Typically, the resonance peak of t-Se is located at ~235 cm^{-1} whereas those of amorphous selenium and monoclinic selenium are centered at ca. 250 cm^{-1} and ca. 260 cm^{-1}, respectively. As shown in Figure S5, only one peak at about 234 cm^{-1} is observed in the frequency region between 200 cm^{-1} and 300 cm^{-1}, which is assigned to the characteristic mode of t-Se. This testifies that the as-prepared t-Se porous products have a high crystal quality and purity, as revealed in the XRD patterns. Note that the XPS and Raman spectra of the flower-like Se pattern are similar.

S6. SEM images of the porous lotus-root-like selenium microspheres.

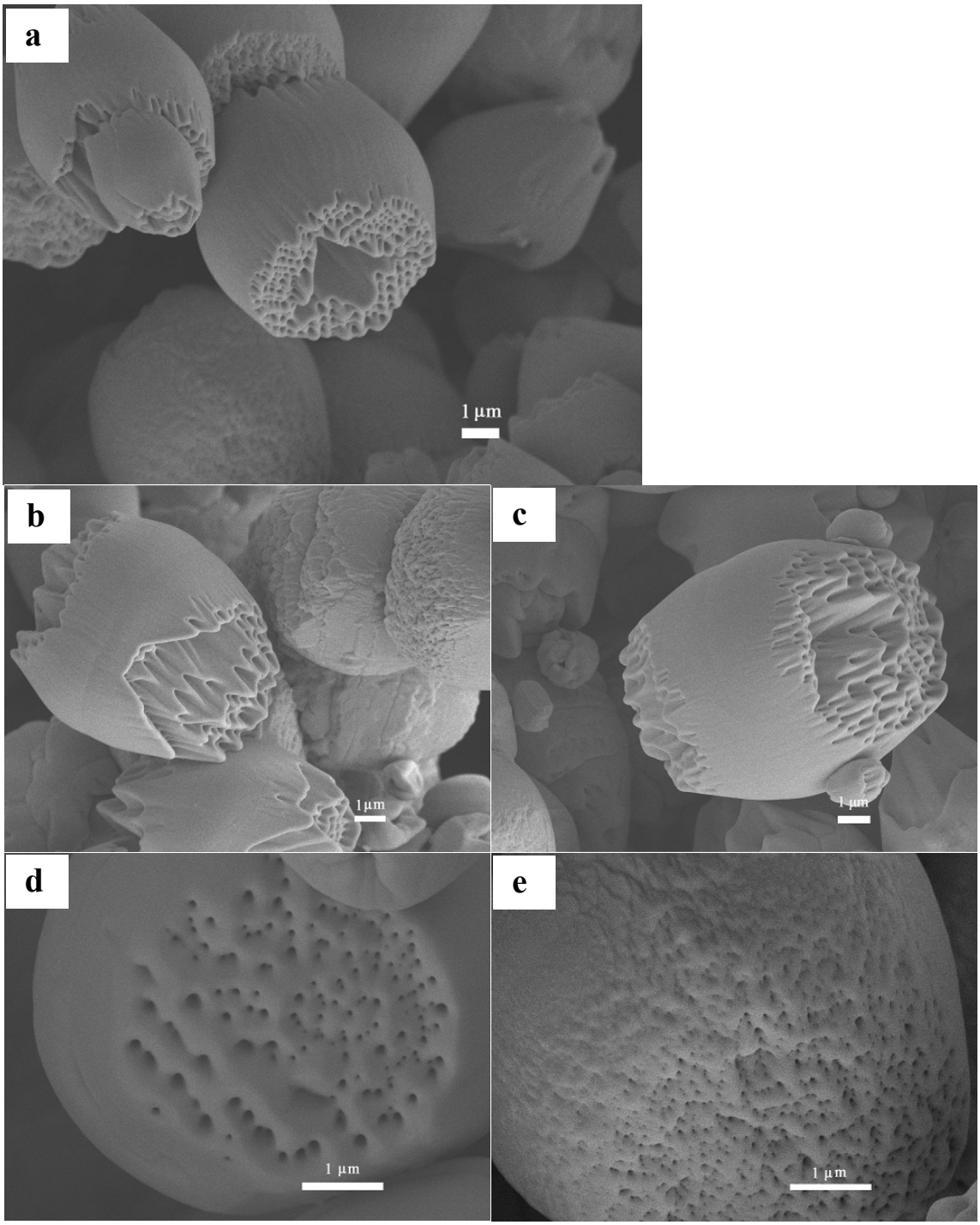

Figure S6. SEM images of porous lotus-root-like microspheres prepared in the presence of 0.254 g Zn foil, 0.358 g Na_2SeO_3, 0.577 g EDTA and 40 mL H_2O at 180 ºC, clearly suggesting the porous structure of the Se materials. Figure S6b, Figure S6c are the side images of some porous lotus-root-like samples. Figure S6d and Figure S6e are the bottom's images of two different lotus-root-like spheres. Note that pores only exist at the bottom of the Se porous lotus-root-like, indicating that the selenium porous microstructures formed along a certain direction.

S7. XRD pattern of porous lotus-root-like selenium microspheres.

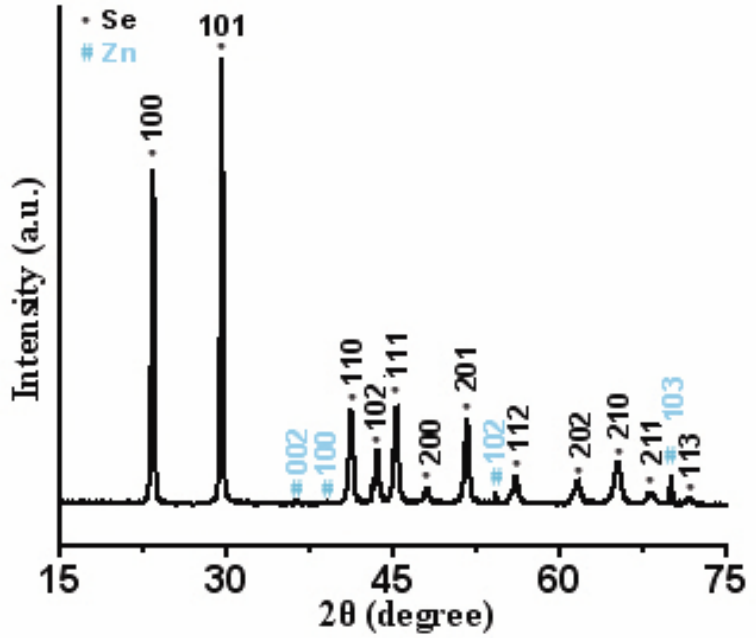

Figure S7. XRD pattern of the as-prepared porous lotus-root-like Se microspheres. Apart from the diffraction peaks of t-Se (JCPDS 06-0362), some weak peaks can be attributed to Zn (JCPDS 04-0831), and the Miller indexes are signed using the cyan font, indicating that the porous Se spheres are grown on the Zn foil.

S8. SEM images of the porous walnut-like spheres

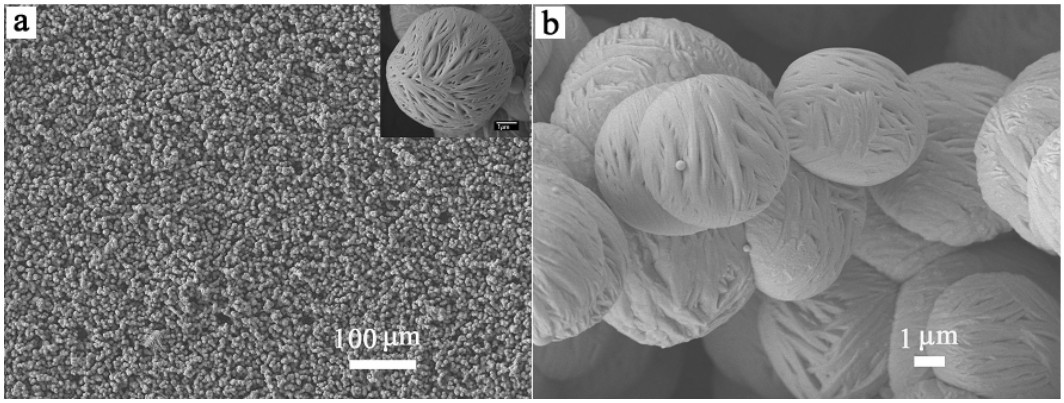

Figure S8. Low magnification (a) and high magnification (b) SEM images of porous walnut-like spheres prepared in the presence of 0.387 g Zn foils, 0.280 g Na_2SeO_3, 0.577 g EDTA and 40 mL H_2O at 150 ºC, indicating the large-scale synthesis of porous walnut-like selenium microstructures.

S9. SEM images of different selenium products prepared in the presence of EDTA at different conditions

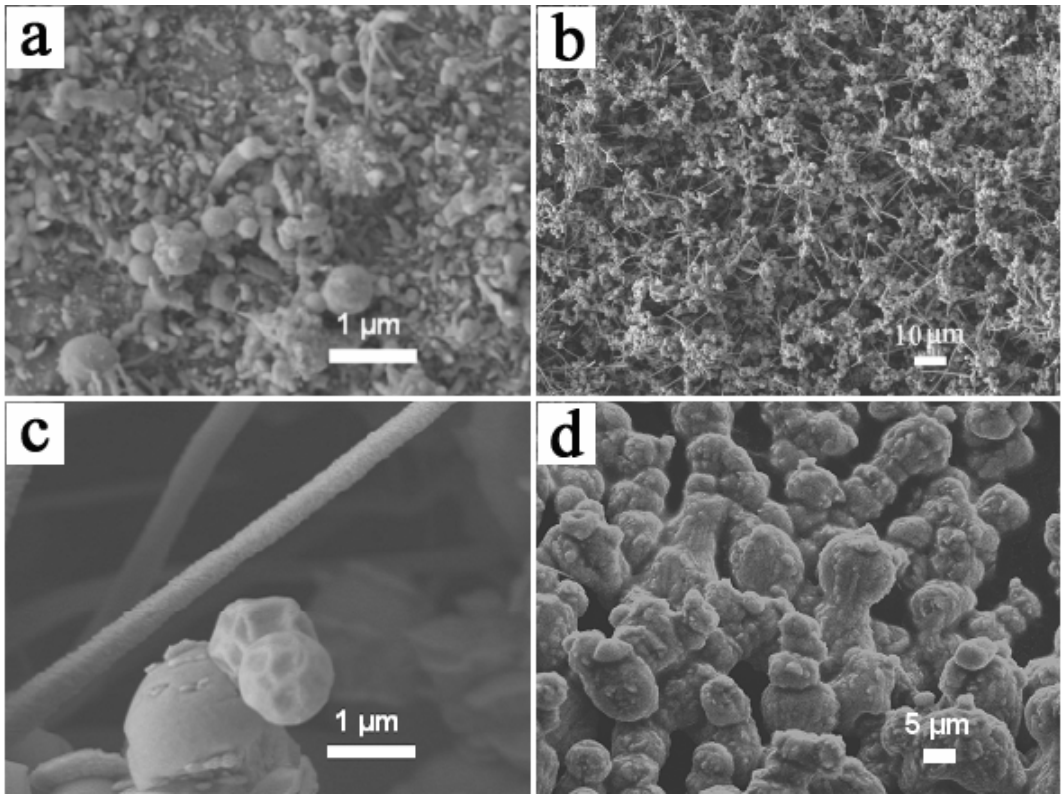

Figure S9. SEM images of four different t-Se samples obtained at different conditions. a) The mixture of particles, spheres and threads, prepared in the presence of 0.254 g Zn foil, 0.358 g Na_2SeO_3, 0.577 g EDTA and 40 mL H_2O at 100 ºC. These samples are obviously different from that of Figure 1c, suggesting that the hydrothermal temperature has a noticeable influence on the shapes of selenium final products. b-c) The mixtures of spheres and wires, prepared in the presence of 0.254 g Zn foil, 0.358 g Na_2SeO_3, 0.250 g EDTA and 40 mL H_2O at 150 ºC, suggesting that the amount of EDTA is important to determine t-Se morphologies. d) Particles fabricated in the presence of 0.358 g Na_2SeO_3, 0.577 g EDTA and 40 mL H_2O at 150 ºC. This further confirms that the coordination of EDTA molecule and Zn^{2+} are essential for controlling the porous morphologies in our solution-phase deposition methods.

S10. The effect of Zn foil on the Se sample's morphology

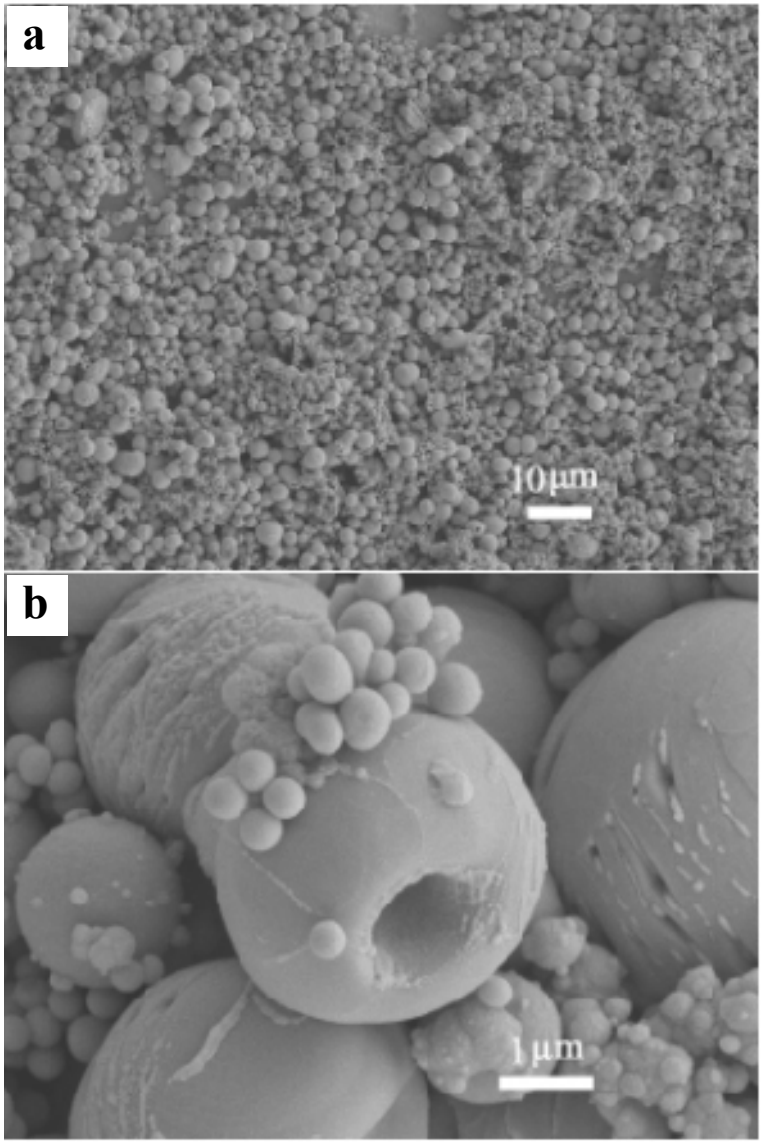

Figure S10. Low magnification (a) and high magnification (b) SEM images of selenium spheres in the presence of 0.189 g $Zn(NO_3)_2$, 0.358 g Na_2SeO_3, 0.577 g EDTA and 40 mL H_2O at 150 ºC, where the Zn foil was replaced by $Zn(NO_3)_2$. As shown in Figure S10, the as-prepared samples are Se spheres, and almost no porous structures can be observed, obviously different from apple-like microspheres displayed in Figure 1c and Figure 1d. This manifests that the Zn substrate and the soft-template, formed through zinc ions adsorbed on Zn foil substrate and EDTA molecules, is very important for the synthesis of the porous Se materials in the solution-phase deposition method.

S11. SEM images of different selenium products prepared in the presence of $N_2H_4 \cdot H_2O$ at different conditions

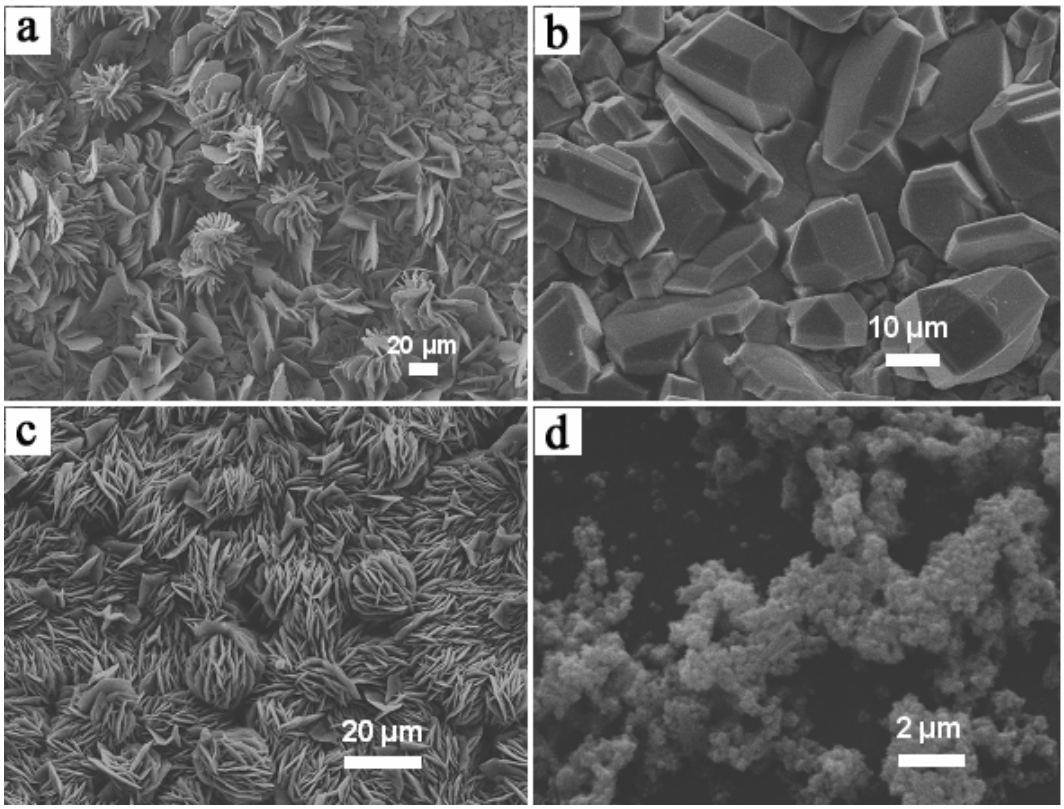

Figure S11-1. SEM images of four different t-Se samples synthesized at different conditions. a) The mixture of flakes, turbine and crystals (the higher SEM image is also shown in Figure S11-2), prepared in the presence of 0.254 g Zn foil, 0.358 g Na_2SeO_3, 0.8 mL $N_2H_4 \cdot H_2O$ and 40 mL H_2O at 120 ºC. This indicates that the hydrothermal temperature has a noticeable influence on the shapes of selenium final products. b) Crystals prepared in the presence of 0.254 g Zn foil, 0.358 g Na_2SeO_3, 0.8 mL $N_2H_4 \cdot H_2O$ and 40 mL H_2O at 90 ºC. This confirms that the hydrothermal temperature are significant in controlling the shapes of selenium final products c) Flakes with irregular arrangements, prepared in the presence of 0.254 g Zn foil, 0.358 g Na_2SeO_3, 0.3 mL $N_2H_4 \cdot H_2O$ and 40 mL H_2O at 150 ºC. This indicates that the amount of $N_2H_4 \cdot H_2O$ has important effect on the Se morphologies and shows that the coordination of $N_2H_4 \cdot H_2O$ and Zn^{2+} are important for the growth of flower-like Se pattern. d) Particles synthesized in the presence of 0.358 g Na_2SeO_3, 0.8 mL $N_2H_4 \cdot H_2O$ and 40 mL H_2O at 150 ºC. This confirms that the coordination of $N_2H_4 \cdot H_2O$ and Zn^{2+} is essential for our solution-phase deposition methods.

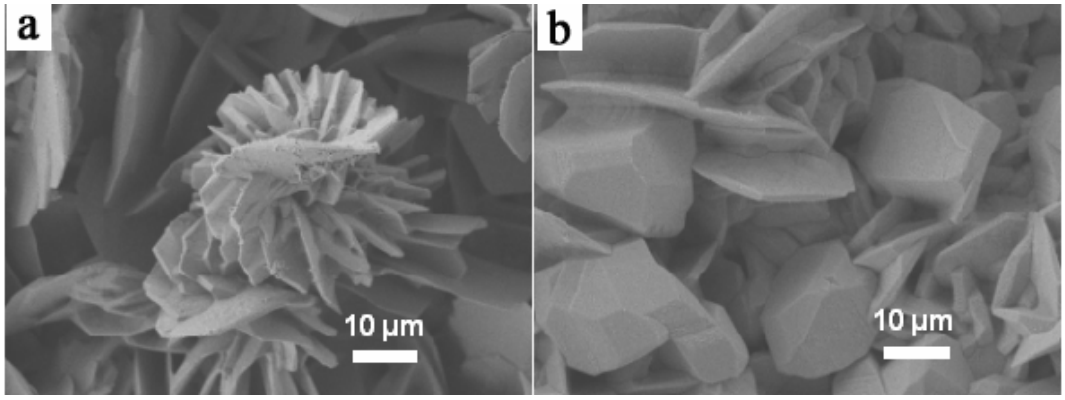

Figure S11-2. High-magnification SEM images of selenium flakes, turbine and crystals, prepared in the presence of 0.254 g Zn foil, 0.358 g Na_2SeO_3, 0.3 mL $N_2H_4 \cdot H_2O$ and 40 mL H_2O at 150 ºC. This shows the coexistence of three kinds of morphologies in the products.

S12. XRD patterns of the intermediates collected in the formation of the porous t-Se apple-like microspheres

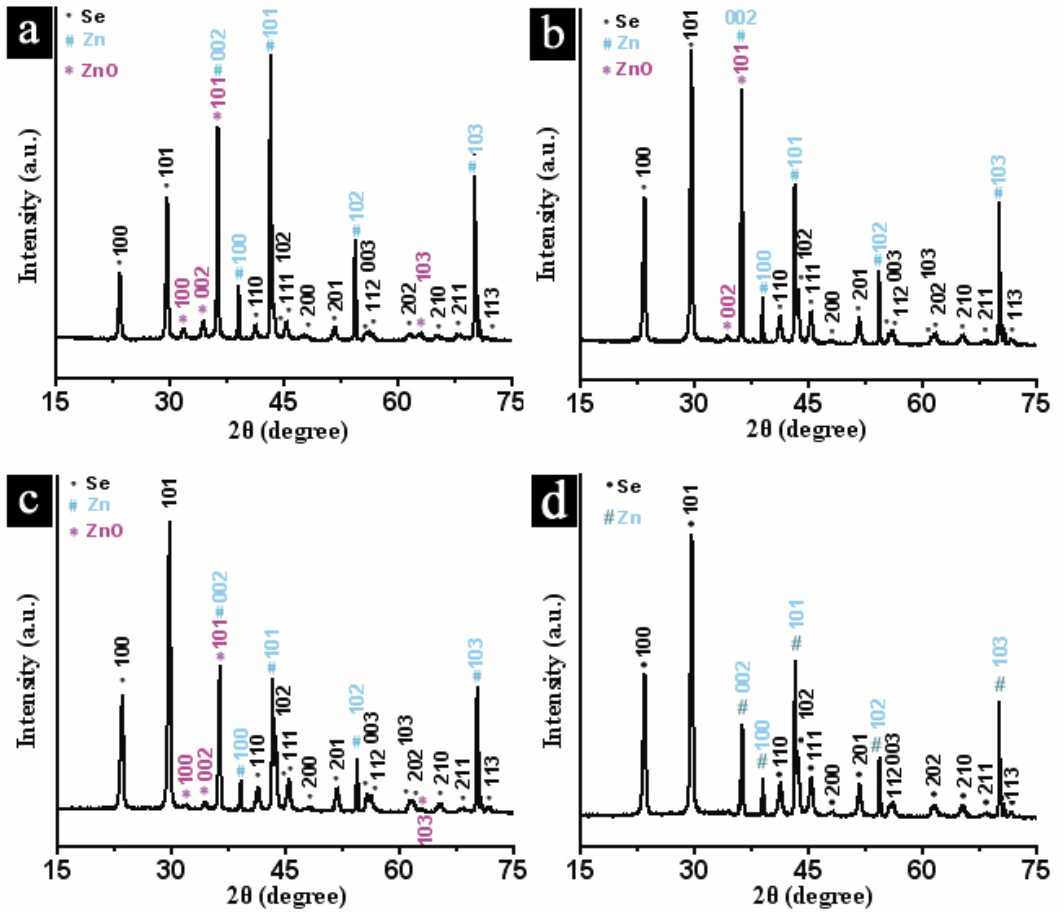

Figure S12. XRD patterns of the interemdiates of porous t-Se microspheres, prepared in the presence of 0.254 g Zn foil, 0.358 g Na_2SeO_3, 0.577 g EDTA and 40 mL H_2O at 150 ºC, collected at different reacting mages. a) 1h; b) 4h; c) 8h; d) 24h.

S13. SEM images of the selenium nanoparticles.

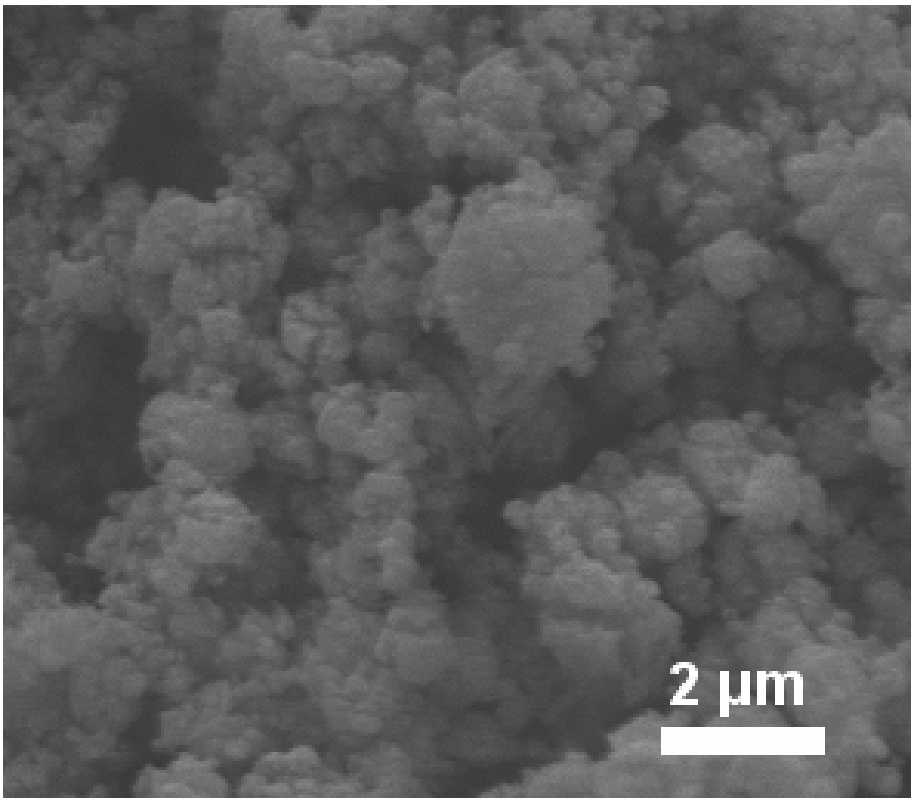

Figure S13. SEM image of the t-Se nanoparticles prepared through hydrothermal treatment of 0.4 g SeO_2, 0.5 mL $N_2H_4 \cdot H_2O$ and 20 mL H_2O for 24 h.

S14. Summary of the shapes of t-Se porous microstructures obtained under various conditions.

Table S1. Summary of the shapes of t-Se porous materials obtained under various conditions.

Amine-containing compounds	Amount of amine-containing compounds	Metal foil	Amount of Na_2SeO_3(g)	Temperature (℃)	Morphologies	SEM images
$N_2H_4 \cdot H_2O$	0.8 ml	0.254 g Zn	0.358	150	Porous flower-like patterns	Figure 1a,b
	0.64 ml	0.242 g Ni	0.358	150	Ear-like microstructures	Figure 4c,d
	0.8 ml	0.254 g Zn	0.358	120	Mixture of flakes, turbine and crystals	Figure S10-1a
	0.8 ml	0.254 g Zn	0.358	90	Crystals	Figure S10-1b
	0.3 ml	0.254 g Zn	0.358	150	Flakes with irregular arrangements	Figure S10-1c
	0.8 ml	0 g	0.358	150	Particles	Figure S10-1d
EDTA	0.577 g	0.254 g Zn	0.358	150	Apple-like microspheres	Figure 1c,d
	0.577 g	0.254 g Zn	0.358	180	Porous lotus-root-like microspheres	Figure 3a,b
	0.577 g	0.254 g Zn	0.358	100	Mixture of particles, spheres and threads	Figure S8a
	0.577 g	0.387 g Zn	0.280	150	Walnut-like spheres	Figure 3c,d
	0.250 g	0.254 g Zn	0.358	150	Mixtures of spheres and wires	Figure S8b,c
	0.577 g	0 g	0.358	150	Particles	Figure S8d
	0.577 g	*	0.358	150	Spheres with no porous structure	Figure S9
	0.577 g	0.242 g Ni	0.358	150	Microspheres	Figure 4a,b

* Zn foil was replaced by 0.189 g $Zn(NO_3)_2$

S15. SEM images of porous Te products prepared by the solution-phase deposition method.

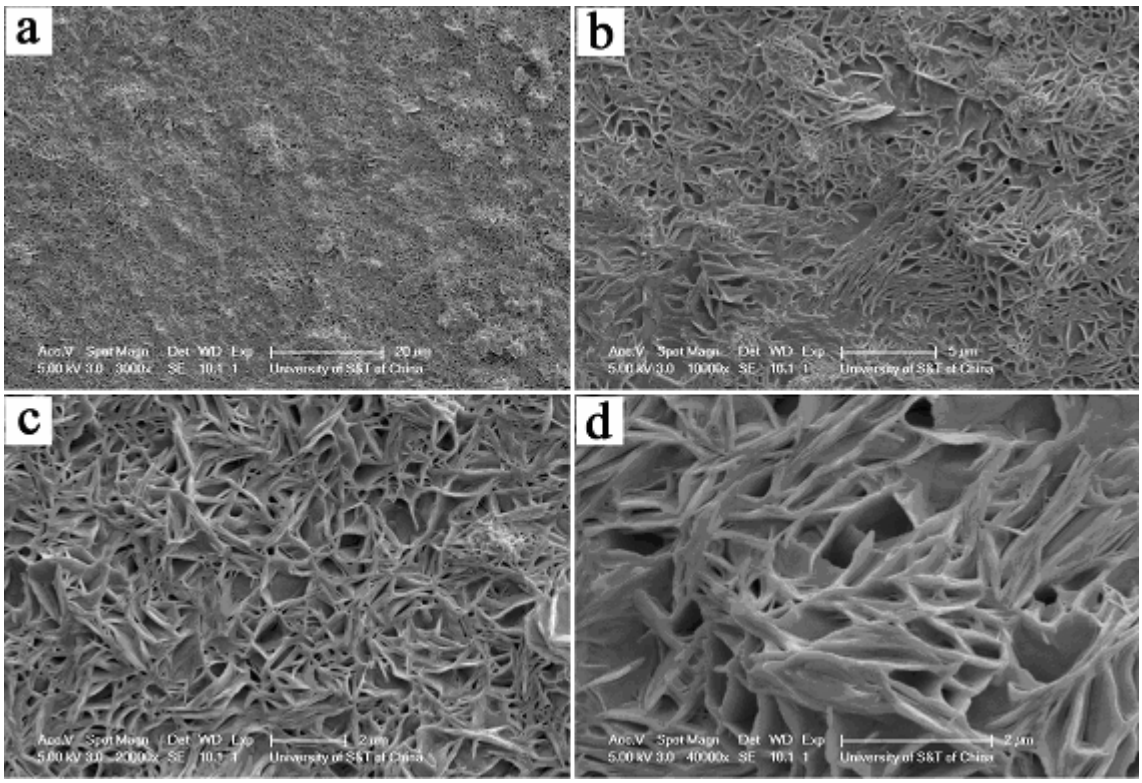

Figure S15. Different-magnification SEM images of porous tellurium samples using the novel solution-phase deposition approach. The samples were prepared in the presence of 0.254 g Zn foil, 0.1 g H_2TeO_3, 0.8 mL $N_2H_4 \cdot H_2O$ and 40 mL H_2O at 150 ºC.